Note

www.tno.nl

To	Erika Neeft	For information
From	Alwina Hoving & Jasper Griffioen	
Subject	Addendum 2 Geochemical characterization of the Watervliet Member - Clay mineralogy and LA-ICP-MS results	
Attachment(s)		

Date
2 February 2026

1. Introduction

This note describes the results of the X-ray diffraction (XRD) analysis of the clay mineral size fraction (<2 µm) and the laser ablation-ICP-MS results of sediment samples from the Watervliet Member from cores taken from borehole KB101 (drilled in 2011 at COVRA, Borsele). The results of other geochemical analyses of these samples are discussed in the report "*Geochemical characterisation of the Watervliet Member and groundwater in Paleogene and other sandy units of Zeeland*"[1]. Due to the fact that the LA-ICP-MS was temporarily out of service and due to the longer interpretation time of the clay mineralogy analysis, these results could not be included in time in the original report. This note discusses these results and serves as an addition to the original report.

The work described in the afore mentioned main report, as well as the work in this addendum and another addendum on isotope analysis of related groundwater samples, received funding from the Ministry of Infrastructure and Water Management.

2. Laser ablation-ICP-MS results

Methods

Laser Ablation-ICP-MS was carried out on two samples to identify the trace elemental content of different minerals encountered. The samples were silty clays which have a similar mineralogical composition with a clay content between 30-40 wt%. The main difference between the samples is that sample 101-100 (101 m below surface, mbs) is a carbonate-rich sample, while sample 101-113 (115 mbs) is a carbonate-poor sample. These samples were embedded in epoxy and polished. 68 spots were analyzed by LA-ICP-MS on these two thin sections. For quantification, the major elements were analyzed on the same spots with Scanning Electron Microscopy with energy dispersive X-ray spectroscopy (SEM-EDX).

Results and discussion

Results from laser-ablation-ICP-MS are plotted in Fig 1. The highest contents of U and Th were found in ilmenite, clay minerals and feldspars with values up to 7 mg/kg and 22 mg/kg, respectively. Pyrite contained around 4 mg/L U but very little Th. The Eu content was highest in feldspars and clay minerals with on average 4 mg/kg and 3 mg/kg, respectively. For Cs, clay minerals, feldspars, and muscovite contained the highest amounts (12-23 mg/kg mineral). Calcite had low contents with respect to these four trace elements. Heavy minerals such as zircon and monazite that were observed in samples from the DAPGEO borehole (Hoving et al., 2025), were not encountered in these thin sections.
When taking into account the content of each mineral in the bulk sediment, the main reservoir of U, Th, Eu and Cs was the clay minerals, with 60-75% of total U/Eu/Th/Cs present in clay minerals (see bar graphs in figure 1). Feldspars contributed around 12-20%, while the other minerals contributed less than 10% to the total budget of each of these trace elements.

[1] Hoving, A., Kivits, T., Griffioen, J. (2024). *Geochemical characterisation of the Watervliet Member and groundwater in Paleogene and other sandy units of Zeeland.* TNO 2024 R12632.

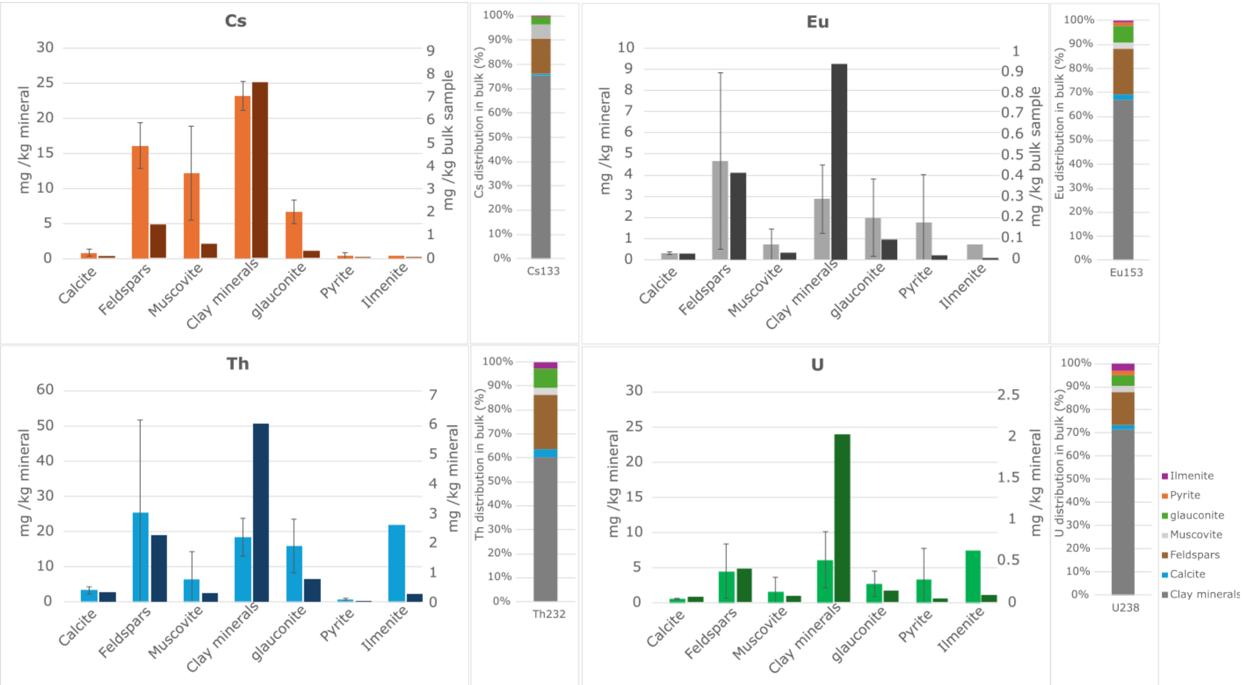

Figure 1. Results from LA-ICP-MS in samples C101-100 and C101-113. The bars in light colors represent the uranium, thorium, europium and cesium content of various minerals as measured by LA-ICP-MS. The elemental content in each mineral is plotted on the left Y-axis. The darker colored bars show the respective element content recalculated in mg/kg bulk sample (plotted on the right Y-axis). For this, the average values of the mineral content in the two samples were used. Error bars represent the standard deviation of the multiple spots measured for each specific mineral. The multi-colored bar on the right side of each graph shows the mineral distribution of each element in the bulk sediment.

3. Clay mineralogy of < 2 µm size fraction

Methods

The clay mineralogy was analyzed by X-Ray Diffraction (XRD, Bruker D8 Advance with DAVINCI). The purification and separation of the clay fraction (< 2 µm) was performed according to the methods described in Zeelmaekers (2011). The mineralogy was measured on oriented clay mounts with three treatments; air dried, after saturation with ethylene glycol, and after heating at 550°C.

Results and discussion

In figure 2 the XRD spectra of all samples after ethylene glycol treatment are shown with the main peaks per clay mineral type indicated. The quantitative results of the clay mineralogy of the < 2 µm size fraction are listed in Table 2. The relative quantities of the various clay minerals vary with depth (Fig. 3). On average smectite was the most abundant clay mineral (45 ± 13 %) of the < 2 µm size fraction, followed by interstratified illite/smectite (I-S) (32 ± 3 %). The illite content was on average 10 ± 2 % and kaolinite accounted for 6 ± 2 % of the < 2 µm size fraction. The chlorite content was below the detection limit for all samples (< 0.5 %). In general, the smectite content within the clay size fraction slightly decreases with depth, while the opposite is the case for the kaolinite content, which slightly increases with depth. A peak in smectite content occurs around 105 mbs.

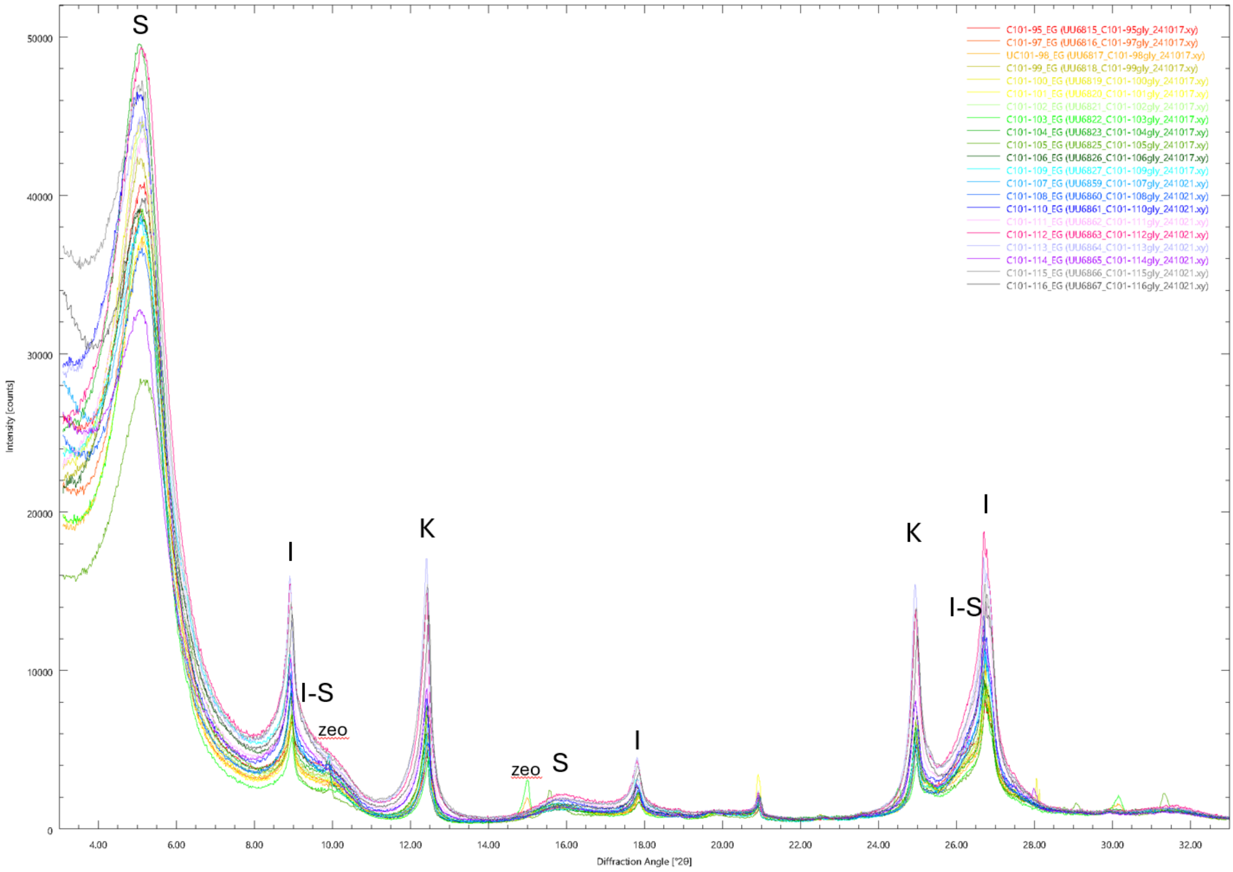

Figure 2. Diffraction pattern of the ethylene glycolated oriented clay fraction (< 2 µm) of all Watervliet Member samples from core KB101. The main peaks of the clay minerals present in these samples are indicated: S = smectite, I = illite, I-S = mixed layered illite-smectite, K = kaolinite, zeo = zeolites clinoptilolite and heulandite.

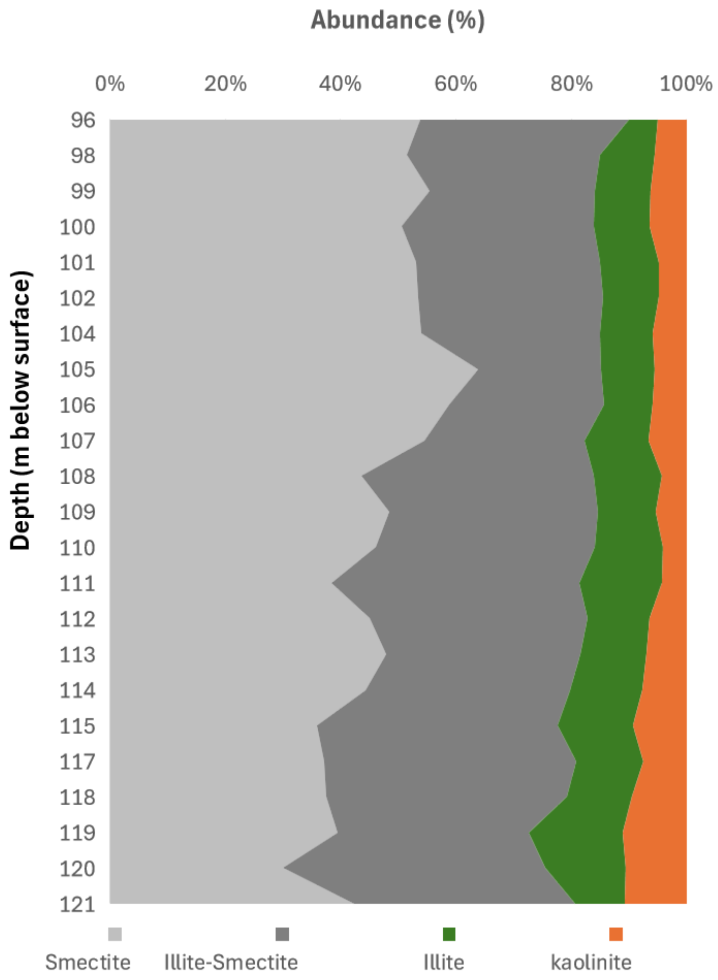

Figure 3. Depth profile of the relative clay mineralogy in the < 2 μm size fraction in samples from borehole KB101.

4. Tables

Table 1 Results from LA-ICP-MS of samples C101-100 (101.2 mbs) and sample C101-113 (115.3 mbs). All values are in mg/kg mineral.

Sample-spot number	Rb85	Sr88	Zr90	Nb93	Mo95	Cs133	La139	Eu153	Pb208	Th232	U238	Targeted mineral
101-100-6	294.8	885.7	162.1	28.5	<DL	22.7	53.1	2.3	18.9	18.9	3.6	Clay minerals
101-100-8	307.9	764.4	165.7	35.2	1.2	24.7	50.8	1.7	25.3	16.2	5.7	Clay minerals
101-100-11	294.7	961.2	166.4	30.6	<DL	23.6	42.1	2.2	37.2	14.7	2.9	Clay minerals
101-100-14	338.5	1143.6	137.4	33	<DL	24.2	76.8	1.2	22.4	12.9	2.5	Clay minerals
101-100-22	276.3	960.2	152.4	26.1	1.1	20.4	64.4	2.3	18.9	13.8	3	Clay minerals
101-100-29	305.4	1294.5	170.1	25.9	<DL	24.5	39.7	1.1	19.2	14.6	2.9	Clay minerals
101-100-35	322.5	1113.2	136.7	22	<DL	24.5	42.9	1.6	19.1	14.9	2.3	Clay minerals
101-100-38	191.5	962.8	79.4	10.8	<DL	12.6	21.8	<DL	20.1	8.8	0.5	Feldspars
101-100-39	216.2	7642.5	142.9	13.5	7.6	16.7	168.2	7.6	1003.6	55.6	8.2	Feldspars
101-100-16	258.3	1500.3	111.3	16.5	<DL	18.7	110.2	1	20	15.5	2.5	Mica (Muscovite)
101-100-21	522.4	222.4	35	14	1.9	15.5	8	0.2	7.1	2.1	0.5	Mica (Muscovite)
101-100-25	346.8	159.8	15.4	31.3	<DL	8.6	7.4	0.4	9.7	1.6	0.3	Mica (Muscovite)
101-100-28	366.6	87.6	4.8	21.3	0.8	7.9	1	0.3	20.7	0.2	<DL	Mica (Muscovite)
101-100-37	181.2	307.4	17.7	17	<DL	2.9	6.3	0.3	20.2	1.8	0.2	Mica (Muscovite)
101-100-7	28.6	320.8	17.8	3.8	<DL	2.6	9.7	0.4	3	2.7	0.5	Carbonate
101-100-24	15	872.1	17.6	1.7	<DL	1.3	10.5	0.4	9.6	2.7	0.6	Carbonate
101-100-2	8.8	185.3	6	0.3	9.7	0.6	12.6	1	80.3	1.4	3.2	Pyrite
101-100-27	11.3	85.4	4.9	0.7	2.7	0.9	3.5	0.2	15.7	0.5	0.4	Pyrite
101-100-36	25	445.7	30.4	0.5	27.4	1.2	62.4	3.8	175.8	0.7	10.2	Pyrite
101-100-40	2.1	502.2	28.5	0.2	15.1	0.2	74.3	5.4	94.6	0.4	8.8	Pyrite
101-100-42	8.5	129.6	210.4	308.5	0.6	0.5	19.4	0.7	96.1	22	7.5	Ilmenite
101-113-11	273.8	93	127.1	23.4	6.6	23.3	49.2	6.7	19.7	17.5	5.8	Clay minerals
101-113-12	260	108.1	145.9	12.6	33.2	19.6	89.1	<DL	69.6	19.4	3.8	Clay minerals
101-113-13	252.7	639.8	131.9	50.3	8.2	20	67.2	4.9	79.1	24.8	8	Clay minerals
101-113-17	307.6	121.2	156.8	18.3	5.6	25.2	55.5	2.8	19.6	16.2	9.1	Clay minerals
101-113-21	312.7	96.9	225.9	22.9	6.9	24.9	48.1	2.3	20.2	17.1	11	Clay minerals
101-113-22	325.9	196.1	175.9	22.5	5.6	26	102.2	5	39.6	33.7	16.4	Clay minerals
101-113-23	259	163.9	125.1	22.8	2.5	21.5	105.7	3.5	30.6	23.1	6.1	Clay minerals
101-113-24	276.1	112.5	140.1	27.6	3.9	22.3	60.7	2.5	18.6	16.8	8.8	Clay minerals
101-113-27	292.8	105	105.5	26.5	3	19.1	31.8	1.7	27.8	11.3	4.6	Feldspars
101-113-7	243.2	69.8	111.1	14.4	1.6	19.6	42.6	2.1	23	17.3	5.5	Mica (Muscovite)
101-113-3	0.6	5.6	0.3	<DL	338	<DL	0.1	<DL	250.2	<DL	<DL	Pyrite
101-113-9	0.9	7.3	1.4	0.1	369.9	0.1	0.4	0	20.9	0.4	0.1	Pyrite
101-113-18	2.6	5.9	2.7	0.1	337	0.2	0.7	0.1	122.6	0.6	0.6	Pyrite
101-113-14	257.5	18.2	88.9	3.7	7	7.9	23.8	0.7	7.4	10.5	1.4	Glauconite
101-113-15	281.3	15	228.7	6.4	2.4	5.5	78.5	3.3	6.7	21.3	3.9	Glauconite

Table 2. Overview of the clay mineralogy of the <2 µm size fraction in the Watervliet Member samples of borehole KB101.

Sample	Depth (mbs)	Smectite (%)	Illite-Smectite (%)	Illite (%)	kaolinite (%)	Chlorite (%)
C101-95	95.7	54	36	5	5	<0.5
C101-97	98.2	51	33	9	5	<0.5
C101-98	99.3	58	30	10	6	<0.5
C101-99	99.9	49	32	9	6	<0.5
C101-100	101.2	54	32	10	5	<0.5
C101-101	102.2	54	33	10	5	<0.5
C101-102	103.8	55	32	9	6	<0.5
C101-103	104.8	77	26	11	7	<0.5
C101-104	105.8	65	30	9	6	<0.5
C101-105	106.8	57	29	12	7	<0.5
C101-106	107.8	39	36	10	4	<0.5
C101-109	109.3	45	34	9	5	<0.5
C101-107	110.3	42	35	11	4	<0.5
C101-108	111.4	32	36	12	4	<0.5
C101-110	112.3	40	34	10	6	<0.5
C101-111	113.3	45	31	11	7	<0.5
C101-112	114.3	39	32	11	7	<0.5
C101-113	115.3	29	33	10	7	<0.5
C101-114	116.8	30	35	9	6	<0.5
C101-115	117.8	30	34	9	8	<0.5
C101-116	118.8	33	28	14	9	<0.5
C101-117	119.7	22	34	10	8	<0.5
C101-118	120.7	36	33	7	9	<0.5

5. References

Hoving. A., Griffioen, J., Kubeneck, J. (2025). Geochemical characterization of Eocene to Miocene deposits of the DAPGEO-2 borehole in Delft. TNO Report TNO 2025 R12729